Supporting Information

Improved Photoelectrochemical Hydrogen Gas Generation on Sb_2S_3 Films Modified with an Earth-Abundant MoS_x Co-Catalyst

Moisés A. de Araújo[1†], Magno B. Costa[1], and Lucia H. Mascaro[1]*

[1]Departamento de Química, Universidade Federal de São Carlos, Rodovia Washington Luiz, km 235, São Carlos – São Paulo, postcode: 13565-905, Brazil

[†]Present address: Instituto de Química de São Carlos, Universidade de São Paulo, Avenida Trabalhador Sancarlense, 400, São Carlos – São Paulo, postcode: 13566-590, Brazil

*Email: lmascaro@ufscar.br

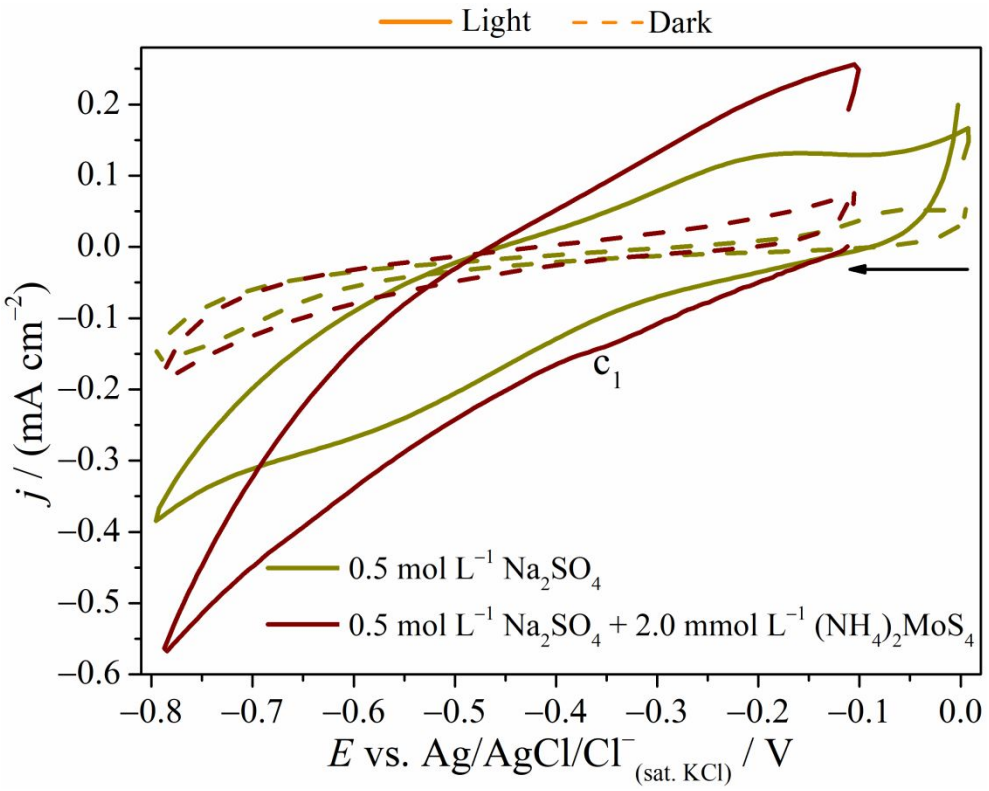

Figure S1. Cyclic voltammograms at a scan rate of 20 mV s^{-1} in the dark and under solar light simulator (AM1.5G and 100 mW cm^{-2}) for PT-Sb_2S_3 film in 0.5 mol L^{-1} Na_2SO_4 pH 5 and 0.5 mol L^{-1} Na_2SO_4 + 2.0 mmol L^{-1} $(NH_4)_2MoS_4$ pH 5.

According to Figure S1, the voltammogram obtained under illumination for PT-Sb_2S_3 film in 0.5 mol L^{-1} Na_2SO_4 + 2.0 mmol L^{-1} $(NH_4)_2MoS_4$ displayed a shoulder cathodic peak c_1 at ca. −0.35 V. Since this peak was not observed in the voltammogram under illumination for PT-Sb_2S_3 film in only 0.5 mol L^{-1} Na_2SO_4, the shoulder peak c_1

was assigned to the PEC reduction of $[MoS_4]^{2-}$ as shown in Equation 1 in the manuscript.

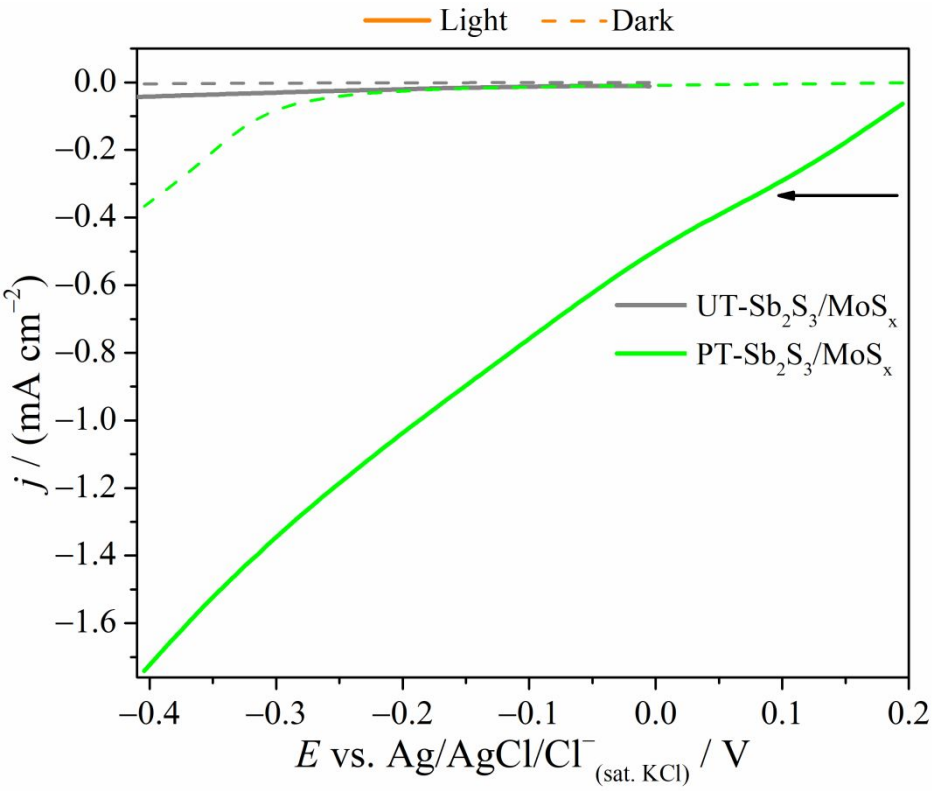

Figure S2. Linear sweep voltammograms at a scan rate of 50 mV s^{-1} in the dark and under solar light simulator (AM1.5G and 100 mW cm^{-2}) for UT-Sb_2S_3/MoS_x and PT-Sb_2S_3/MoS_x films. The electrolyte was an N_2-saturated solution of 1.0 mol L^{-1} H_2SO_4 at pH 0.6. The MoS_x was photoelectrodeposited on the UT-Sb_2S_3 and PT-Sb_2S_3 films for 10 min.

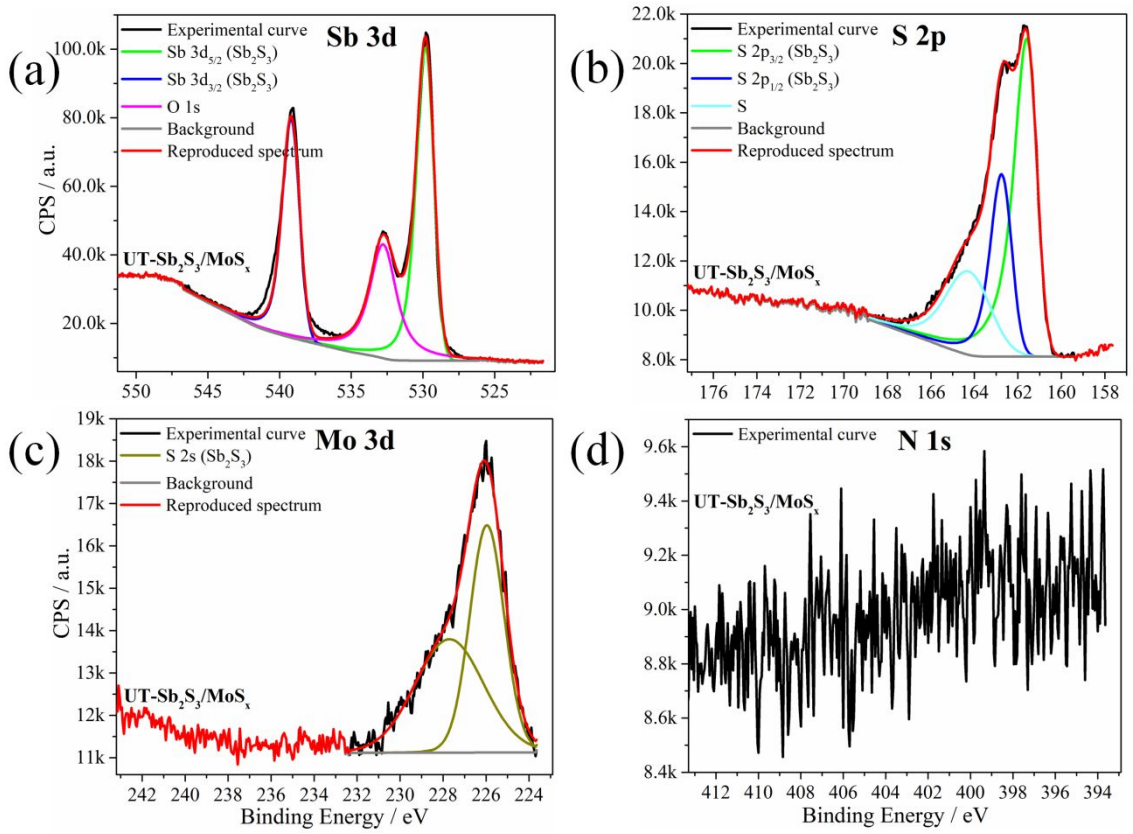

Figure S3. High-resolution XPS spectra of (a) Sb 3d, (b) S 2p, (c) Mo 3d, and (d) N 1s core levels for UT-Sb_2S_3/MoS_x film. The MoS_x was photoelectrodeposited on the UT-Sb_2S_3 film for 10 min.

From Figure S3a, the Sb 3d spectrum for the UT-Sb_2S_3/MoS_x film presented photoemission peaks at 529.6 (Sb $3d_{5/2}$) and 539.0 eV (Sb $3d_{3/2}$), which are assigned to Sb^{3+} in Sb_2S_3.[1] Additionally, the spectrum displayed a photoemission peak at 532.8 eV

(O 1s) and that is probably associated with adsorbed water.[2] The S 2p spectrum for the UT-Sb_2S_3/MoS_x film (cf. Figure S3b) displayed photoemission peaks at 161.4 (S $2p_{3/2}$) and 162.6 eV (S $2p_{1/2}$) which are characteristic for S^{2-} in Sb_2S_3.[3] The additional peak at 163.9 eV is probably attributed to residual elemental sulphur[4] on the Sb_2S_3 films' surface and this may have come from the sulphurisation step. For the Mo 3d spectrum in Figure S3c, one can observe the photoemission peaks at 226.0 and 227.7 eV for S 2s,[5] which are possibly assigned to Sb_2S_3. The N 1s spectrum (see Figure S3d) did not display any photoemission signal. This result was already expected for the UT-Sb_2S_3/MoS_x film since the Sb_2S_3 film was not subjected to N_2 plasma treatment. We only observed photoemission peak in the N 1s region for the Sb_2S_3 films once treated under N_2 plasma, for more details the reader is referred to our latest work[6] and the discussion of Figure 4 in this manuscript.

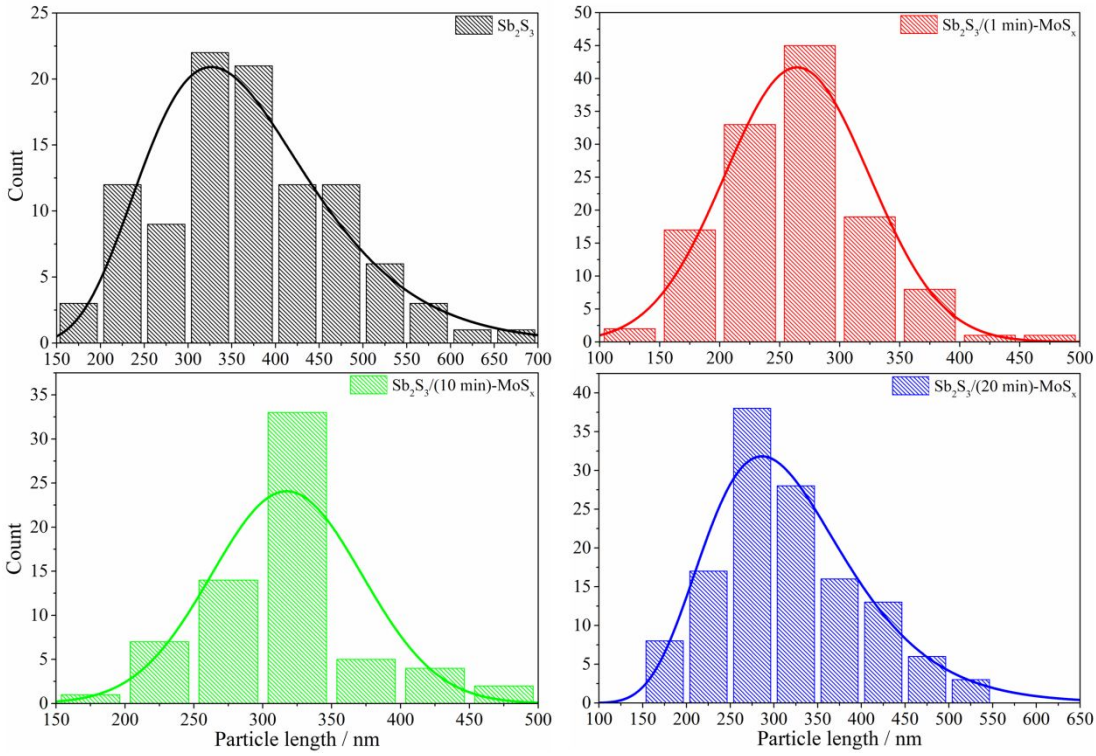

Figure S4. Particle size distribution histograms for PT-Sb_2S_3 and PT-Sb_2S_3/(1, 10, or 20 min)-MoS_x films.

To obtain the particle size distribution, histograms were constructed and are displayed in Figure S4. We employed the ImageJ[7,8] (version 1.51j8) software to measure the length of up to 130 particles from the SEM micrographs. According to Figure S4, the estimated particle length for bare PT-Sb_2S_3 film was 325 nm, whilst the particle length for PT-Sb_2S_3 films superficially modified with MoS_x photoelectrodeposited for 1, 10, and 20 min was ca. 275, 325, and 275 nm, respectively.

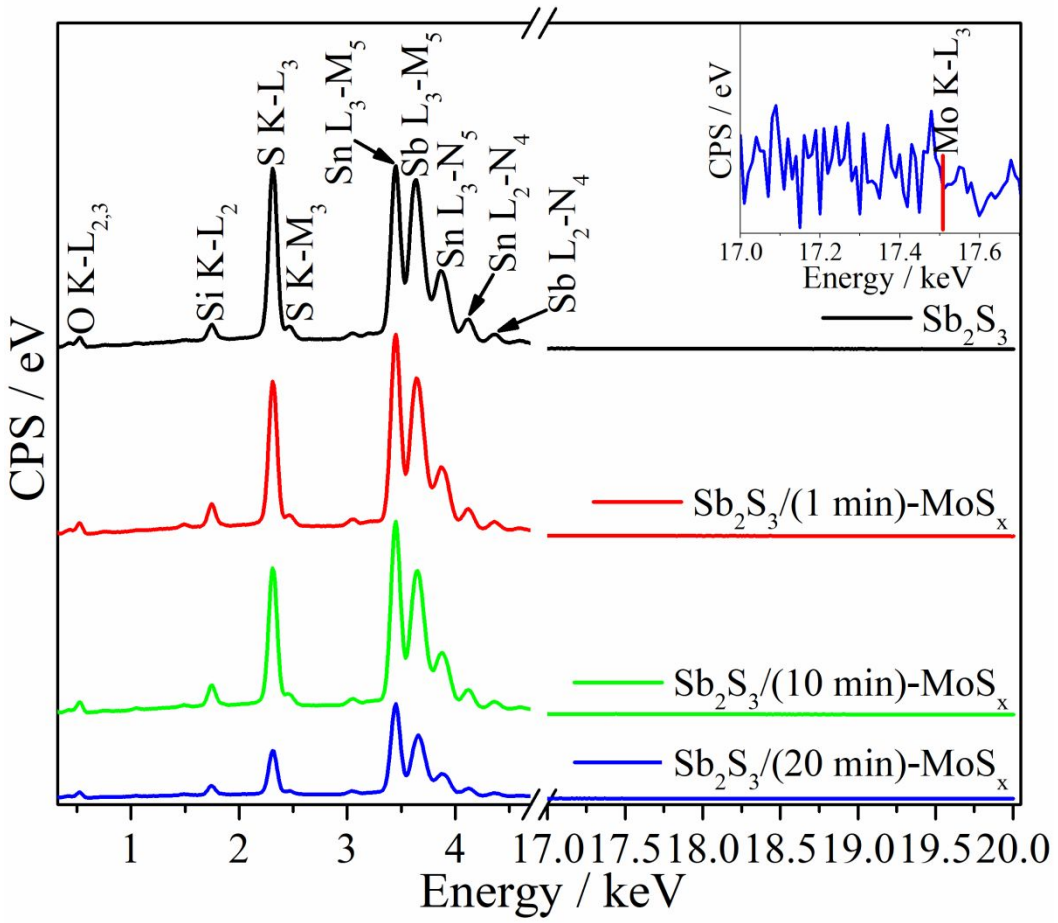

Figure S5. EDS spectra for PT-Sb_2S_3 and PT-Sb_2S_3/(1, 10, or 20 min)-MoS_x films. The characteristic X-ray emission lines energies of the elements were assigned using Grieken and Markowicz's database.[9] The peaks assigned to the O, Si, and Sn elements are from the substrate (glass/FTO).

Table S1. Atomic percentage of Sb and S obtained from the EDS spectra for PT-Sb_2S_3 and PT-Sb_2S_3/(1, 10, or 20 min)-MoS_x films.

Sample	Atomic percentage / %		Atomic ratio
	Sb	S	S/Sb
Sb_2S_3	21	34	1.6
Sb_2S_3/(1 min)-MoS_x	17	30	1.8
Sb_2S_3/(10 min)-MoS_x	15	29	1.9
Sb_2S_3/(20 min)-MoS_x	12	23	1.9

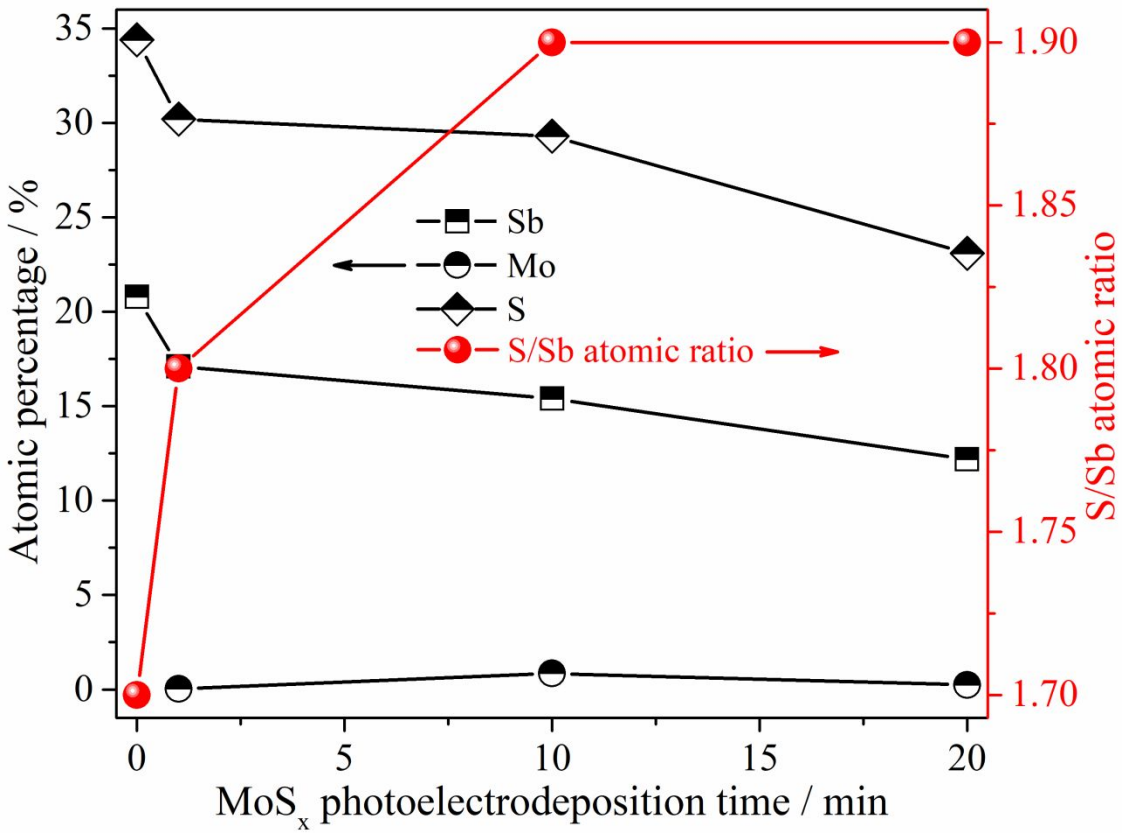

Figure S6. Atomic percentage of Sb, Mo and S, and S/Sb atomic ratio obtained from the EDS spectra for PT-Sb_2S_3 and PT-Sb_2S_3/(1, 10, or 20 min)-MoS_x films.

Table S2. Binding energy assignment from the high-resolution XPS spectra for PT-Sb_2S_3 and PT-Sb_2S_3/(1 or 10 min)-MoS_x films.

Core level		Binding energy / eV			Assignment	Ref.
		PT-Sb_2S_3	PT-Sb_2S_3/(1 min)-MoS_x	PT-Sb_2S_3/(10 min)-MoS_x		
Sb 3d	Sb $3d_{3/2}$	540.4	539.9	539.2	Sb_2S_3	10,11
	Sb $3d_{5/2}$	531.0	530.5	529.8	Sb_2S_3	10,11
	O 1s	532.1	532.2	531.9	Adsorbed O_2, H_2O, etc.	12
Mo 3d	Mo $3d_{3/2}$	-	232.9	233.2	MoS_2	13–15
		-	236.3	236.2	MoO_3 and/or MoO_xO_y	14,16–18
	Mo $3d_{5/2}$	-	229.8	230.0	MoS_2	13–15
		-	233.2	233.0	MoO_3 and/or MoO_xO_y	14,16–18
	S 2s	232.8	-	-	S-N bond	19–21
		-	226.1	226.6	MoS_2	14
S 2p	S 2p	168.5	-	-	S-N bond	19,20,22
		169.5	-	-	S-N bond	19,20,22
	S $2p_{3/2}$	-	161.4	161.8	S^{2-} in MoS_x	23,24
		-	162.6	163.1	S_2^{2-} in MoS_x	23,24
	S $2p_{1/2}$	-	162.4	162.8	S^{2-} in MoS_x	23,24
		-	163.6	164.1	S_2^{2-} in MoS_x	23,24
N 1s	N 1s	401.7	399.5	398.9	S-N bond	20,21,25
	Mo $3p_{3/2}$	-	395.8	396.1	MoS_2	14

Table S3. Percentage error values for each circuit element to fit the complex-plane impedance diagrams obtained at −0.2 V vs. $Ag/AgCl/Cl^-_{(sat.\ KCl)}$ and under solar light simulator (AM1.5G and 100 mW cm^{-2}) for PT-Sb_2S_3 and PT-Sb_2S_3/(1 min)-MoS_x films. The electrolyte was an N_2-saturated solution of 1.0 mol L^{-1} H_2SO_4 at pH 0.6.

	Percentage error[a] / %	
Circuit element	PT-Sb_2S_3	PT-Sb_2S_3/(1 min)-MoS_x
R_s	0.95	0.60
$R_{ct,sc}$	11	8.9
$R_{ct,d}$	5.4	5.2
Q_{sc}	6.8	3.8
$\alpha_{f,sc}$	5.7	1.4
Q_d	2.1	9.8
$\alpha_{f,d}$	0.32	0.70

[a]The fit of the complex-plane impedance diagrams for PT-Sb_2S_3 and PT-Sb_2S_3/(1 min)-MoS_x films delivered chi-squared (χ^2) values of 0.00048296 and 0.00022833, respectively.

References

1. Birchall, T.; Connor, J. A.; Hillier, L. H. High-Energy Photoelectron Spectroscopy of Some Antimony Compounds. *J. Chem. Soc. Dalt. Trans.* **1975**, 0, 2003–2006. DOI: 10.1039/dt9750002003.

2. He, G.-H.; Liang, C.-J.; Ou, Y.-D.; Liu, D.-N.; Fang, Y.-P.; Xu, Y.-H. Preparation of Novel Sb_2O_3/WO_3 Photocatalysts and Their Activities under Visible Light Irradiation. *Mater. Res. Bull.* **2013**, 48, 2244–2249. DOI: 10.1016/j.materresbull.2013.02.055.

3. Zhang, Z.; Zhao, J.; Xu, M.; Wang, H.; Gong, Y.; Xu, J. Facile Synthesis of Sb_2S_3/MoS_2 Heterostructure as Anode Material for Sodium-Ion Batteries. *Nanotechnology* **2018**, 29, 335401. DOI: 10.1088/1361-6528/aac645.

4. Lindberg, B. J.; Hamrin, K.; Johansson, G.; Gelius, U.; Fahlman, A.; Nordling, C.; Siegbahn, K. Molecular Spectroscopy by Means of ESCA II. Sulfur Compounds. Correlation of Electron Binding Energy with Structure. *Phys. Scr.* **1970**, 1, 286–298. DOI: 10.1088/0031-8949/1/5-6/020.

5. Moulder, J. F.; Stickle, W. F.; Sobol, P. E.; Bomben, K. D. *Handbook of X-ray Photoelectron Spectroscopy*; Perkin-Elmer Corporation, 1992.

6. de Araújo, M. A.; Mascaro, L. H. Plasma Treatment: A Novel Approach to Improve the Photoelectroactivity of Sb_2S_3 Thin Films to Water Splitting. *ChemElectroChem* **2020**, 7, 2325–2329. DOI: 10.1002/celc.202000496.

7. Abràmoff, M. D.; Magalhães, P. J.; Ram, S. J. Image Processing with ImageJ. *Biophotonics Int.* **2004**, 11, 36–42.

8. Schneider, C. A.; Rasband, W. S.; Eliceiri, K. W. NIH Image to ImageJ: 25 Years of Image Analysis. *Nat. Methods* **2012**, 9, 671–675. DOI: 10.1038/nmeth.2089.

9. Grieken, R. E. V.; Markowicz, A. A. *Handbook of X-Ray Spectrometry*; Marcel Dekker, Inc., 2002.

10. Morgan, W. E.; Stec, W. J.; Wazer, J. R. V. Inner-Orbital Binding-Energy Shifts of Antimony and Bismuth Compounds. *Inorg. Chem.* **1973**, 12, 953–955. DOI: 10.1021/ic50122a054.

11. Zakaznova-Herzog, V. P.; Harmer, S. L.; Nesbitt, H. W.; Bancroft, G. M.; Flemming, R.; Pratt, A. R. High Resolution XPS Study of the Large-Band-Gap Semiconductor Stibnite (Sb_2S_3): Structural Contributions and Surface Reconstruction. *Surf. Sci.* **2006**, 600, 348–356. DOI: 10.1016/j.susc.2005.10.034.

12. Chow, P. K.; Singh, E.; Viana, B. C.; Gao, J.; Luo, J.; Li, J.; Lin, Z.; Elías, A. L.; Shi, Y.; Wang, Z.; Terrones, M.; Koratkar, N. Wetting of Mono and Few-Layered WS_2 and MoS_2 Films Supported on Si/SiO_2 Substrates. *ACS Nano* **2015**, 9, 3023–3031. DOI: 10.1021/nn5072073.

13. Stevens, G. C.; Edmonds, T. Electron Spectroscopy for Chemical Analysis

Spectra of Molybdenum Sulfides. *J. Catal.* **1975**, 37, 544–547. DOI: 10.1016/0021-9517(75)90190-6.

14. Ganta, D.; Sinha, S.; Haasch, R. T. 2-D Material Molybdenum Disulfide Analyzed by XPS. *Surf. Sci. Spectra* **2014**, 21, 19. DOI: 10.1116/11.20140401.

15. Wang, X.; Cormier, C. R.; Khosravi, A.; Smyth, C. M.; Shallenberger, J. R.; Addou, R.; Wallace, R. M. In Situ Exfoliated 2D Molybdenum Disulfide Analyzed by XPS. *Surf. Sci. Spectra* **2020**, 27, 014019. DOI: 10.1116/6.0000153.

16. Werfel, F.; Minni, E. Photoemission Study of the Electronic Structure of Mo and MO oxides. *J. Phys. C Solid State Phys.* **1983**, 16, 6091–6100. DOI: 10.1088/0022-3719/16/31/022.

17. Escalera-López, D.; Niu, Y.; Park, S. J.; Isaacs, M.; Wilson, K.; Palmer, R. E.; Rees, N. V. Hydrogen Evolution Enhancement of Ultra-Low Loading, Size-Selected Molybdenum Sulfide Nanoclusters by Sulfur Enrichment. *Appl. Catal. B Environ.* **2018**, 235, 84–91. DOI: 10.1016/j.apcatb.2018.04.068.

18. Benoist, L.; Gonbeau, D.; Pfister-Guillouzo, G.; Schmidt, E.; Meunier, G.; Levasseur, A. X-Ray Photoelectron Spectroscopy Characterization of Amorphous Molybdenum Oxysulfide Thin Films. *Thin Solid Films* **1995**, 258, 110–114. DOI: 10.1016/0040-6090(94)06383-4.

19. Mengel, P.; Grant, P. M.; Rudge, W. E.; Schechtman, B. H.; Rice, D. W. X-Ray-Photoelectron-Spectroscopy Determination of the Valence Band Structure of Polymeric Sulfur Nitride, $(SN)_x$. *Phys. Rev. Lett.* **1975**, 35, 1803–1806. DOI: 10.1103/PhysRevLett.35.1803.

20. Brant, P.; Weber, D. C.; Ewing, C. T.; Carter, F. L. The Application of Gas Phase and Solid State X-ray Photoelectron Spectroscopy to the Investigation of Derivatives Containing the Repeating SN Unit. *Synth. Met.* **1980**, 1, 161–173. DOI: 10.1016/0379-6779(80)90007-7.

21. Sharma, J.; Downs, D. S.; Iqbal, Z.; Owens, F. J. X-Ray Photoelectron Spectroscopy of S_2N_2 and the Solid State Polymerization of S_2N_2 to Metallic $(SN)_x$. *J. Chem. Phys.* **1977**, 67, 3045. DOI: 10.1063/1.435268.

22. Sharma, J.; Iqbal, Z. X-Ray Photoelectron Spectroscopy of Brominated $(SN)_x$ and S_4N_4. *Chem. Phys. Lett.* **1978**, 56, 373–376.

23. Vrubel, H.; Hu, X. Growth and Activation of an Amorphous Molybdenum Sulfide Hydrogen Evolving Catalyst. *ACS Catal.* **2013**, 3, 2002–2011. DOI: 10.1021/cs400441u.

24. Zhang, T.; Huang, J.; Xia, Y.; Zhao, R.; Sun, B.; Xiong, J.; Tao, B.; Wang, H.; Zhao, Y. A High-Efficiency Electrocatalyst for Hydrogen Evolution Based on Tree-Like Amorphous MoS_2 Nanostructures Prepared by Glancing Angle Deposition. *J. Solid State Chem.* **2020**, 286, 121255. DOI: 10.1016/j.jssc.2020.121255.

25. Banister, A. J.; Hauptman, Z. V.; Passmore, J.; Wong, C.-M.; White, P. S. Poly(Sulphur Nitride): An Assessment of the Synthesis from Trichlorocyclotri(Azathiene) and Trimethylsilyl Azide. *J. Chem. Soc. Dalt.*

Trans. **1986**, 2371–2379. DOI: 10.1039/DT9860002371.